Nucleate Pool Boiling Heat Transfer to Al_2O_3-Water and TiO_2-Water Nanofluids on Horizontal Smooth Tubes with Dissimilar Homogeneous Materials

M. M. Sarafraz* **and S. M. Peyghambarzadeh**
Department of Chemical Engineering, Mahshahr Branch,
Islamic Azad University, Mahshahr, Iran

Original scientific paper
Received: October 5, 2011
Accepted: July 24, 2012

Nucleate pool boiling heat transfer coefficients of Al_2O_3-water and TiO_2-water nanofluids have been experimentally measured on three horizontal tubes with different materials and similar roughness under atmospheric pressure. Results revealed that the presence of nanoparticles in the base fluid leads to an increase in pool boiling heat transfer coefficients on stainless steel and brass tubes in contrast to copper tube. The effect of different materials on excess temperature around the surface of the tubes has also been investigated. In addition, experimental investigations on the effect of different nanoparticles on nucleate boiling heat transfer have been conducted at volumetric concentrations of 0.1 %, 0.5 %, and 1 % of nanoparticles. Results indicated that the presence of nanoparticles have no effect on the pool boiling heat transfer coefficient for the copper tube. Variations of surface excess temperature for the copper tube were higher in comparison with that of the other tubes tested.

Key words:
Pool boiling, nanofluids, heat transfer, excess temperature, horizontal smooth tube, Al_2O_3, TiO_2

Introduction

Recent advances in nanotechnology applications have allowed development of a new class of liquids termed nanofluids, first used by a group at Argonne National Laboratory USA[1] to describe liquid suspensions containing nanoparticles with thermal conductivities, orders of magnitude higher than the base liquids, and with sizes significantly smaller than 100 nm. The augmentation of thermal conductivity could provide the basis for a major innovation for the intensification of heat transfer, which is pertinent to several industrial sectors including transportation, power generation, micro-manufacturing, chemical and metallurgical industries, as well as heating, cooling, ventilation, and the air-conditioning industries.[2] Literature findings regarding pool boiling of nanofluids can be summarized as follows: The use of nanofluids application in the field of heat transfer was introduced by Choi.[3] Das *et al.*[4] studied nucleate pool boiling heat transfer of Al_2O_3-water nanofluids on the surface of a horizontal cylindrical cartridge. The presence of nanoparticles negatively affected the boiling performance and the negative impact became more pronounced when the nanoparticle concentration was increased. Similar results were found in the later study by Das *et al.*[5] using smaller cartridges. These authors believed that the lower pool boiling performance was related to changes of the heater's surface characteristics. You *et al.*[6] studied pool boiling heat transfer of silica-water and alumina-water nanofluids at sub-atmospheric pressure. Results showed that the presence of nanoparticles increased the values of the critical heat flux (CHF). Witharana[7] studied the effect of gold nanoparticles on boiling heat transfer of water under atmospheric pressure and found a noticeable increase in nucleate boiling heat transfer. Vassllo *et al.*[8] investigated the pool boiling heat transfer behavior of silica-water nanofluids on a horizontal Ni-Cr wire under atmospheric pressure. Although their experiments illustrated a 200 % CHF increase, no significant heat transfer coefficient enhancement was observed. Tu *et al.*[9] obtained a significant enhancement in both boiling heat transfer coefficient and critical heat flux with Al_2O_3 water nanofluids. Due to these contradictions, more research on the effect of nanoparticles on the pool boiling heat transfer coefficient are required for better understanding.[10–13]

Experimental

Experimental setup

As shown in Fig. 1, used were three similar tubes (in terms of roughness and geometrical sizes) of dimensions: Length 450 mm; Outer diameter 20 mm. The cubic test chamber was a stainless

*Corresponding Author:
Email: mohamadmohsensarafraz@gmail.com, Tel: +989166317313;
Peyghambarzadeh@gmail.com; Tel: +989123241450

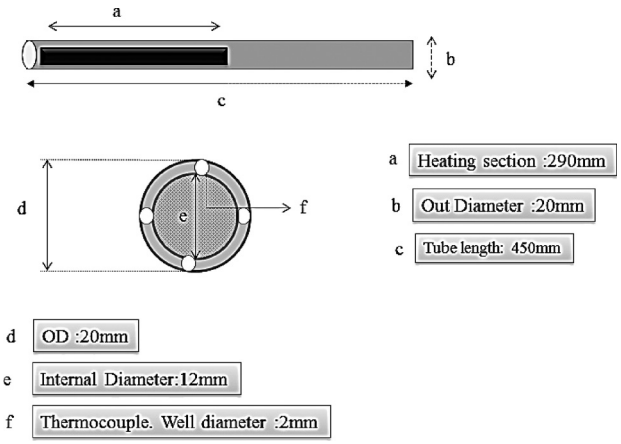

F i g . 1 – *Schematic and dimensions of heating section*

steel made vessel with inside dimensions of 450 mm × 150 mm × 150 mm. The chamber was heavily isolated using industrial glass wool to prevent heat loss from the sides. To measure the cylinder surface temperature, four K-Type thermocouples, 150 mm in length and 2 mm in diameter, were installed near the surface at 12, 3, 6, 9 o'clock position of the cross section of each tube. To minimize the contact thermal resistance, high quality silicon paste was injected through the thermocouple wells. Arithmetic average of the four readings was considered as surface temperature. A regular DC power source was used to supply power to the central heater and unit. To prevent the vapor from escaping, a vertical condenser was used. More details are given in Figs. 1–3, respectively. Noticeably, in this work, similar to some earlier works,[2,7,13] all the heat generated by the central heater is considered to be radially transferred to the solution and no axial or radial heat loss is considered. In this regard, the test chamber was heavily isolated and therefore no heat loss was considered throughout the vessel.

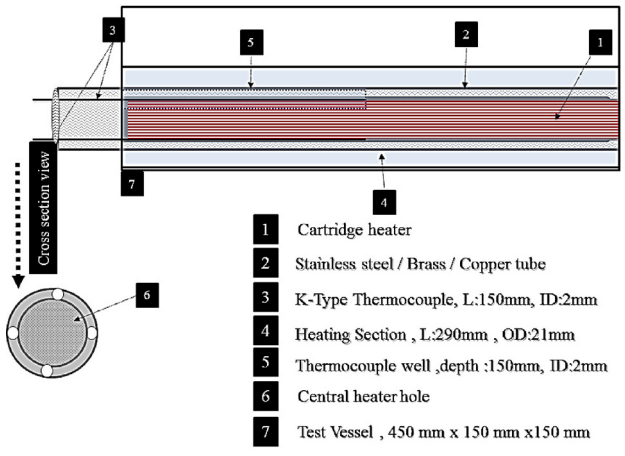

F i g . 2 – *Details of cartridge heater and cross-sectional view*

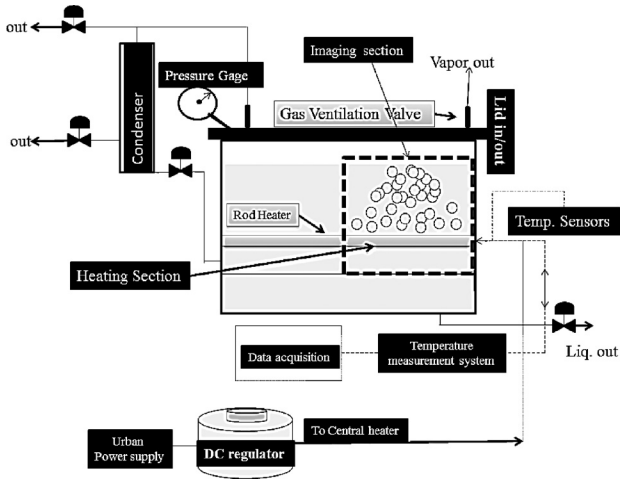

F i g . 3 – *Schematic of the experimental apparatus*

Plenary experimental procedure

In each experimental run, each tube was polished several times with wet emery paper (roughness approximately 0.03–0.04 μm) to achieve apparent smoothness. Profilometer images show that the roughness of each tube's surface could be considered smooth at approximately 0.034 μm.[20] In this research, a contact profilometer was used. In brief, the use of the profilometer proceeded as follows: A diamond stylus was moved vertically in contact with a cylinder surface and then moved laterally across the cylinder for a specific distance at specific contact force. A profilometer can measure small surface variations in vertical stylus displacement as a function of position. The profilometer used in this research (P6-Roll KLA Tencor) could measure small vertical features ranging from 10 nanometers to 1 millimeter in height. The height position of the diamond stylus generates an analog signal, which is converted into a digital signal stored, analyzed and displayed. The radius of diamond stylus ranges from 20 nanometers to 25 μm, and the horizontal resolution is controlled by the scan speed and data signal sampling rate. The stylus tracking force can range from less than 1 to 50 milligrams. Fig. 4 represents the surface roughness for copper, stainless steel and brass tubes. As seen, the surfaces have closely similar roughness and can be considered similarly.

To prepare the nanofluid with desired concentration, nanoparticles were homogeneously dispersed into pure water. Each time, a magnetic stirrer was used to mix the nanoparticles uniformly for about 3.5 hrs. To control the range of pH, simultaneous with mixing, a Digital pH meter (Omega, PHH-830) was employed. Respectively, one hour before adding nanofluids into the test vessel, an ultrasonic device (Hielscher) was used to stabilize

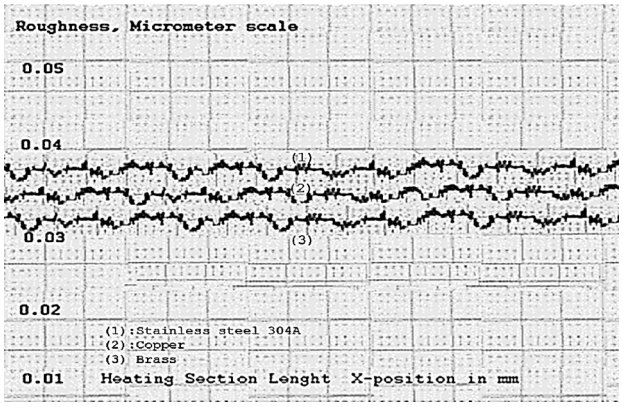

F i g . 4 – *Surface roughness of cylinder tubes provided by profile meter*

and homogenize the particles into the base fluid. A two-step statistical counting was also done before running and finishing the experiments in order to measure the average nanoparticles size. Results of the two-step counting were almost similar to each other. Fig. 5 presents the particle size for Al_2O_3 and TiO_2 nanoparticles.

As shown in Fig. 5, average particle sizes for Al_2O_3 and TiO_2 were 48 nm and 52 nm respectively.

To calculate the real surface temperature, eq. (1) was used to mathematically estimate the surface temperature values.

$$T_s - T_{thm} = U \cdot I \cdot \frac{\ln\left(\frac{r_o}{r_i}\right)}{2\pi \cdot K \cdot L} \qquad (1)$$

Where: T_s is real surface temperature, T_{thm} is arithmetic average of four installed thermocouples, U is heater voltage, and I is current of heater, r_o and r_i are outer and inner diameter of tube respectively, L is effective length, and K is thermal conductivity of the tube. The boiling heat transfer coefficient α is calculated by the following equation:

$$\alpha = \frac{q/A}{(T_s - T_b)_{ave.}} \qquad (2)$$

T_b is the saturation temperature of the tested liquid. To ensure accuracy of thermocouple readings, calibration with pure water was done before running the experiments. After calibration, the entire system including the central heater and the inside of the test vessel were cleaned and the test liquid was introduced. Then the vacuum pump was turned on and the pressure of the system was kept low approximately at 10 kPa for about eight hours to allow all the dissolved gases, especially the dissolved air, to escape from the test liquid. Following this, the vessel band heater was switched on and the

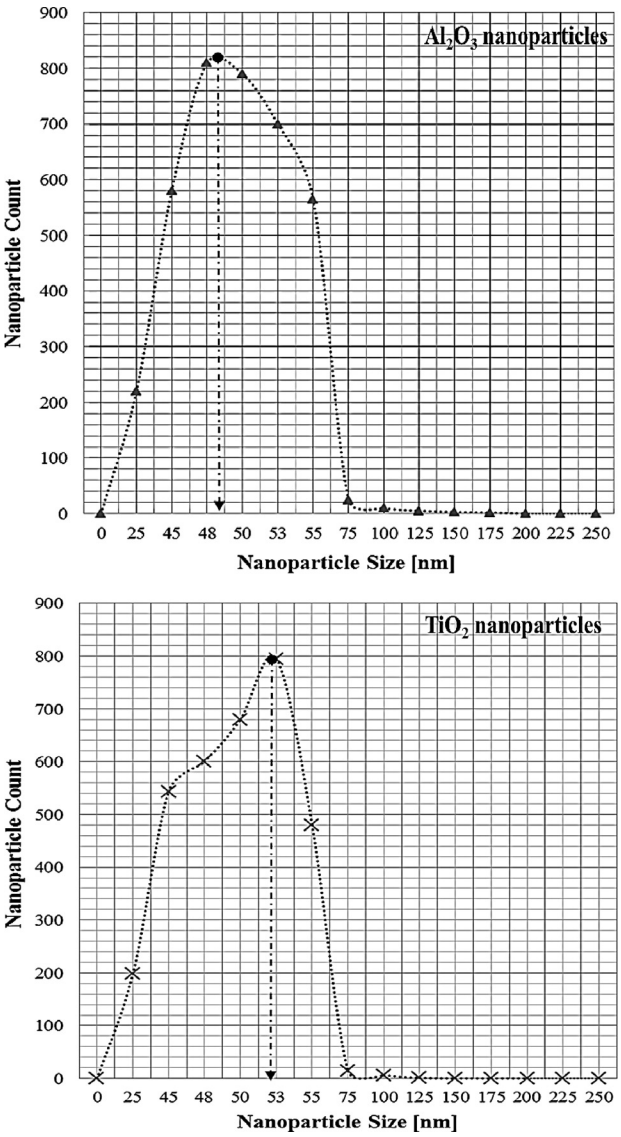

F i g . 5 – *Nanoparticle size distribution of Al_2O_3 and TiO_2 after sonication*

temperature of the system was allowed to rise to saturation temperature. This procedure presents a homogeneous condition right through. Then power was slowly supplied to the rod heater and increased gradually to a constant predetermined value. Data acquisition systems were simultaneously switched on to record the required parameters including the central heater temperature, bulk temperature, heat flux. All experimental runs were carried out with decreasing heat flux to eliminate the hysteresis effect. To maintain the constant heat flux, as seen in Fig. 2, a DC voltage regulator was used to prevent fluctuations in the alternate current. Therefore, the constant heat flux at each voltage exhibits no fluctuations. Some runs were repeated more than three times to ensure the reproducibility of the experiments and measured experimental data. After each run, the tube was changed with a dissimilar tube

and all the steps repeated. Additionally, nanoparticles were substituted to survey the influence of different nanoparticles on different tube materials. Noticeably, in each experimental run, the height of the tested liquid was about 15 mm above the upper surface of each tube in order to conserve the pool boiling mode and prevent changing the nanofluid concentration due to the base fluid evaporation (water).

Uncertainty prediction

To measure the uncertainty of each experimental run, the mathematical mean square method was used. According to heat flux estimating correlation:

$$q'' = \frac{U \cdot I}{2\pi \cdot r_o \cdot L} = \frac{W}{2\pi \cdot r_o \cdot L} \tag{3}$$

Experimental uncertainty is obtained from the following equation:

$$\Delta q'' = \sqrt{\left(\frac{\partial q''}{\partial w}\cdot \Delta w\right)^2 + \left(\frac{\partial q''}{\partial r_o}\cdot \Delta r_o\right)^2 + \left(\frac{\partial q''}{\partial L}\cdot \Delta L\right)^2} \tag{4}$$

With regard to Table 1, value for $\Delta q''$ will be estimated.

Table 1 – *Values for* Δw, Δr_o, ΔL

No.	Parameter	Δ	Unit
1	Δw	6.5	Watt
2	Δr_o	0.2	mm
3	ΔL	0.01	mm

Accordingly, pool boiling heat transfer coefficient uncertainty, according to the traditional assumption $\alpha = f(q'', T)$ and obtained $\Delta q''$ by eq. (4) is obtained by the following equation:

$$\Delta \alpha = \sqrt{\left(\frac{\partial \alpha}{\partial q''}\cdot \Delta q''\right)^2 + \left(\frac{\partial q''}{\partial T}\cdot \Delta T\right)^2} \tag{5}$$

In this research, ΔT equals ±0.3 K due to accuracy of each thermocouple and $\Delta q''$ equals 1.25 % according to eq. (4). Furthermore, uncertainty of estimating the heat transfer coefficient equals ± 8.1 %.

Results and discussions

To validate the apparatus as well as the experimental procedure and operation of temperature measurement system, data for distilled water was compared with nanofluids. Likewise, this comparison was repeated for various dissimilar tubes. These data are kept as a reference for further comparisons with experimental data. For better understanding, experimental heat transfer coefficients of pure water for three different tubes are given at Fig. 6. Fig. 6 presents the pool boiling heat transfer coefficient for stainless steel, brass and copper tubes. For different tubes, the results are closely similar. However, copper tube heat transfer coefficient is the poorest heat transfer coefficient while the stainless steel tube is the highest.

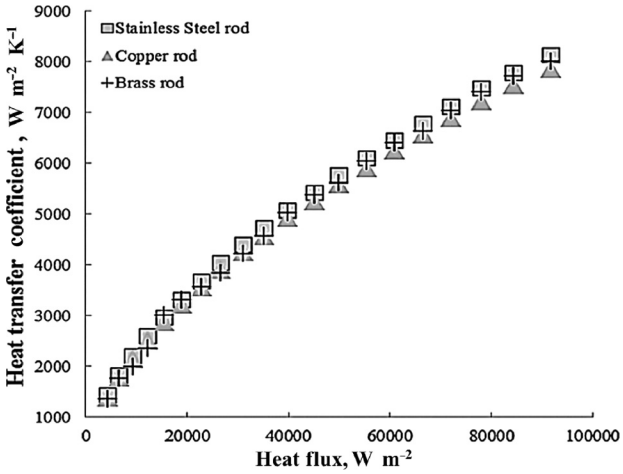

Fig. 6 – *Comparison of pool boiling heat transfer coefficients for water*

According to eq. (2), lower superheat wall temperature leads to higher heat transfer coefficient. Therefore, with a rough comparison between Fig. 6 and 7 and also considering eq. (2), it is found that:

$$\alpha_{Stainless\ steel} > \alpha_{Brass} > \alpha_{Copper} \tag{6}$$

Respecting to eq. (6), for a clear understanding, the excess temperatures (Surface temperature-saturation temperature which is also called wall superheat temperature) of each tube have been compared in Fig. 7.

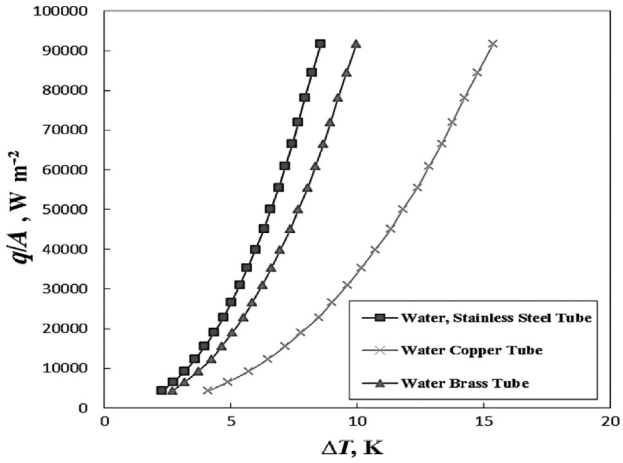

Fig. 7 – *Comparison of excess temperature of each tube for pure water*

Results for stainless steel tube show that the rate of increase of pool boiling heat transfer coefficient in the presence of nanoparticles is higher than other tubes. Clearly, increased nanofluids concentration leads to increased heat transfer coefficients, which is shown in Fig. 8.

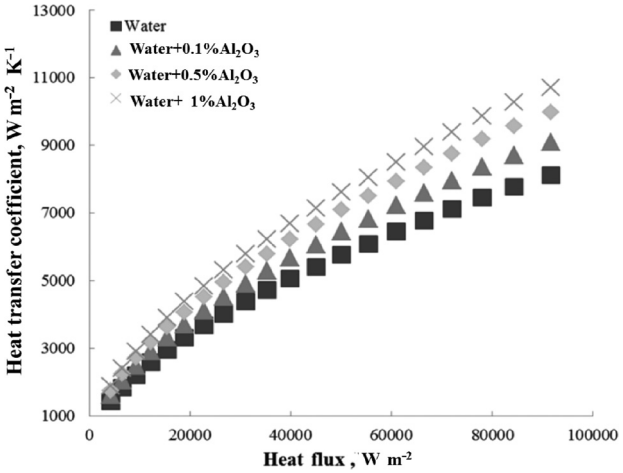

F i g . 8 – *Experimental heat transfer coefficients of Al_2O_3 nanofluids on stainless steel tube*

Figs. 9 and 10 similarly show the experimental pool boiling heat transfer coefficient on brass and copper tube respectively. Unlike stainless steel, for the copper tube the heat transfer coefficient deteriorates with increased concentration of nanoparticles.

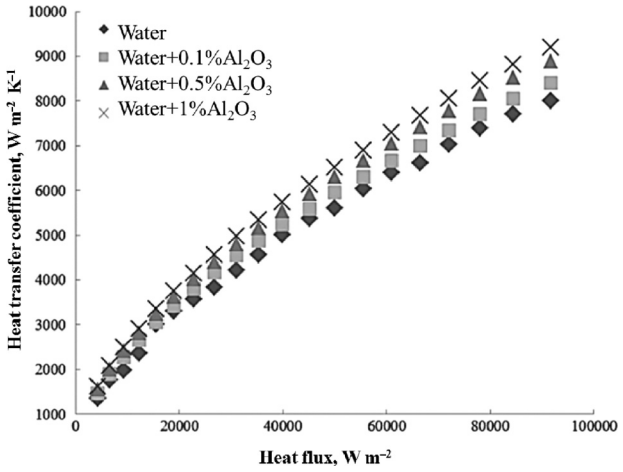

F i g . 9 – *Experimental heat transfer coefficient Al_2O_3 nanofluids on Brass tube*

For clearly representing the influence of different nanoparticles on pool boiling heat transfer, TiO_2 nanoparticle was selected to be substituted with Al_2O_3. Table 2 presents some physical properties of these nanoparticles.

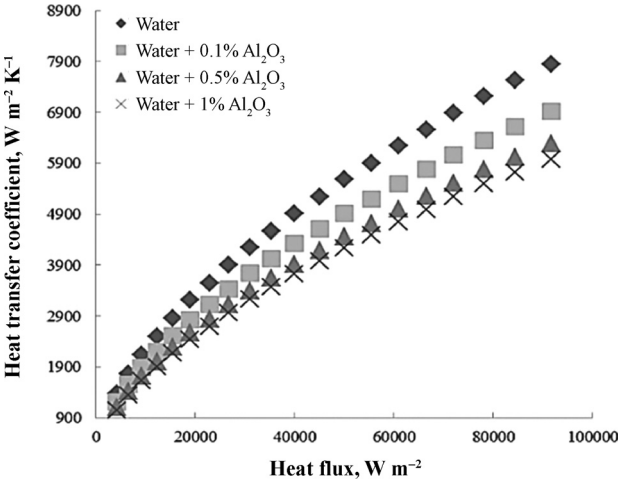

F i g . 1 0 – *Experimental heat transfer coefficient Al_2O_3 nanofluids on copper tube at various concentrations of Al_2O_3*

T a b l e 2 – *Physical properties of tested nanoparticles*

Nano-particle	Density, g cm^{-3}	Molar mass, g mol^{-1}	Conductivity, W m^{-1} K^{-1}	Mean particle size
Al_2O_3	4.05	101.96	30	48 nm
TiO_2	4.23	79.9	12.1	52 nm

In general, the contradicting results observed during the boiling of nanofluids could be due to the complex nature of boiling heat transfer. During boiling several parallel mechanisms of heat transfer, namely phase change, natural convection due to surface tension, micro convection due to bubble departure, Marangoni convection due to surface tension gradient along the bubble surface are present. The presence of solid particles in nanofluid not only changes the thermal conductivity substantially, but could also alter the surface tension of the fluid and the surface properties of the heater. The effect of nanoparticles could depend on a number of parameters like composition, shape, size, concentration agglomeration etc. Therefore, it is too early to predict a generalized heat transfer behavior of nanofluids. A large number of systematic experiments under controlled conditions are needed to ascertain the effect of each parameter of the nanofluid on boiling heat transfer. However, due to the significant influence of nanoparticles on surface roughness, the excess temperature (wall superheat temperature) decreases. The main reason for this phenomenon refers to the fact that due to increase of thermal conductivity in result of nanoparticle deposition, especially around the surface, the conduction heat transfer mechanism is improved and heat

transfer mechanism will occur conveniently. Besides, the presence of deposition particularly around the heating surface changes surface roughness locally and helps generate more bubble columns. Furthermore, the generated heat of the heater will be transferred to bulk of solution conveniently in comparison to the case without nanoparticles, and surface temperature profile is degraded too. Subsequently, the heat transfer coefficient increases. Additionally, to ensure validation of obtained results, the experimental results were cross checked using Cooper proposed correlation:[12]

$$\alpha = 0.55 \cdot p_r^{0.12 - 0.434 (\log p_r)} \cdot \cdot [-0.434 \log (p_r)]^{-0.55} \cdot M^{-0.5} \cdot q''^{0.67} \quad (7)$$

Where p_r is reduced pressure, q'' is corresponding heat flux, and M is molecular mass. Results of pool boiling heat transfer coefficient for TiO_2 nanoparticles are shown in Figs. 11–13 for stainless steel, brass and copper tubes respectively. As seen in Figs. 11 and 12, similar to Al_2O_3, an increased concentration of nanoparticles leads to increased heat transfer coefficient around the stainless steel and brass tubes. Increased values for stainless steel are higher than for the brass tube.

In contrast to stainless steel and brass tube, the boiling heat transfer coefficient significantly deteriorated on the copper tube experiments. The main reason for this phenomenon is the fact that copper has the highest thermal conductivity compared to the other materials, and the temperature of copper surface is also higher than that of stainless steel or brass tubes. The presence of nanoparticles around the copper tube surface changes the surface roughness and contact angle clearly exhibiting heat transfer deterioration despite the high thermal conductivity of copper. Therefore, nanoparticles have a negative effect on boiling heat transfer around the copper tube. In this regard, more experiments are needed to show the influence of nanoparticles precisely.

It is not recommended to use nanoparticles for enhancing the boiling heat transfer coefficient around copper smooth surfaces. For confirmation, Fig. 14 shows the variations of excess temperature in comparison with nucleate boiling heat transfer coefficient for various tubes with the presence of nanoparticles simultaneously.

Fig. 15 typically represents the excess temperatures (wall superheat temperatures) of used tubes at pool boiling heat transfer of 1 % volumetric TiO_2 nanofluid. Briefly speaking, due to the lower thermal conductivity of stainless steel in comparison with brass and copper tubes, the heating section

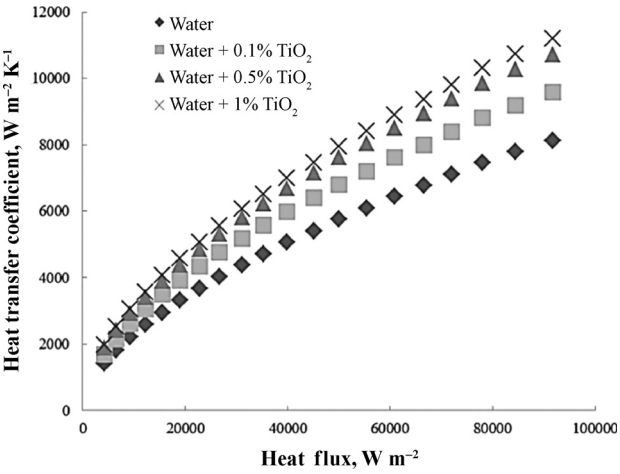

Fig. 11 – *Experimental heat transfer coefficient for TiO_2 nanofluids on stainless steel tube*

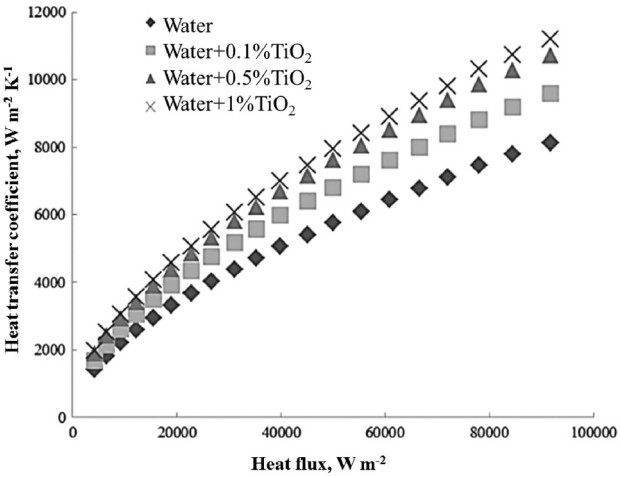

Fig. 12 – *Experimental heat transfer coefficient for TiO_2 nanofluids on brass tube*

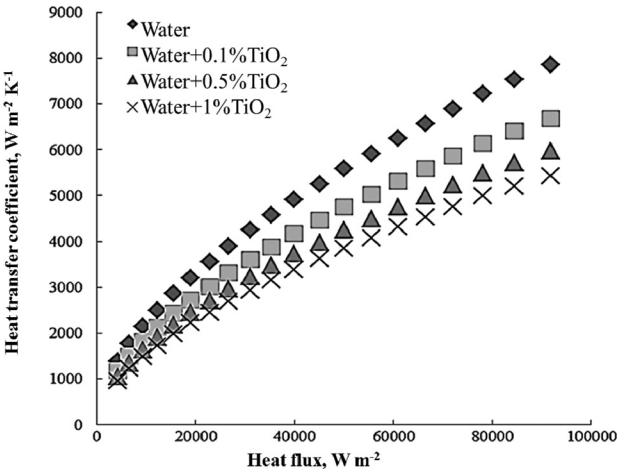

Fig. 13 – *Experimental heat transfer coefficient for TiO_2 nanofluids on copper tube*

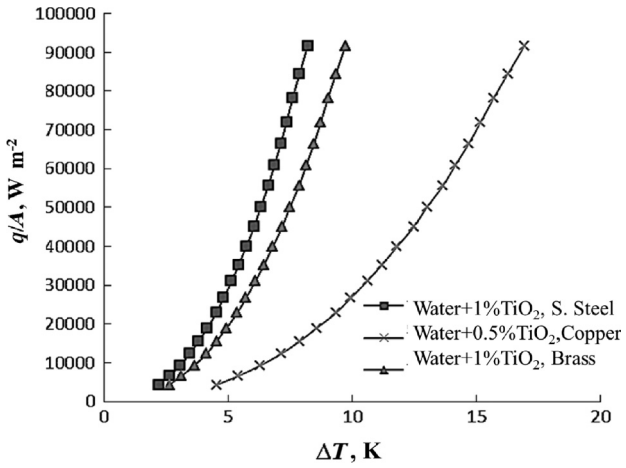

F i g . 1 4 – *Excess temperatures of dissimilar tubes at different heat fluxes*

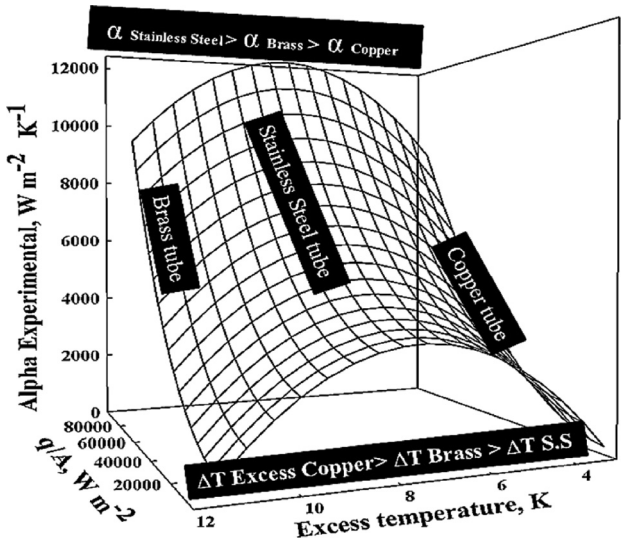

F i g . 1 5 – *Status of heat transfer coefficient, excess temperature and heat flux for different tube materials*

surface temperature is lower relative to the other tubes and with regard to eq. (1), the nucleate boiling heat transfer coefficient around stainless steel is higher than that of brass and copper tubes. However, for the copper tube, due to very high thermal conductivity and strict dependence of its conductivity on temperature, the heat transfer coefficient is deteriorated and wall super heat temperature around the copper tube rises in comparison with other materials.

Although for CHF, in earlier works, the higher wall super heat temperature, the higher CHF has been reported but in lower heat fluxes and at initial steps of boiling, lower wall super heat is desired owing to the higher heat transfer rates which is truly observable in this work.

Conclusion

Experimental investigation of pool boiling heat transfer has been conducted on different tubes with similar dimensions for different concentrations of Al_2O_3 and TiO_2 nanofluids. For stainless steel and brass tubes, the presence of nanoparticles significantly enhanced the pool boiling heat transfer coefficients. In contrast, heat transfer coefficients deteriorated around the copper tube due to its higher thermal conductivity in comparison with the other tubes. Additionally, TiO_2 in comparison with Al_2O_3 enhances the pool boiling heat transfer coefficient for stainless steel and brass tubes, but decreases the pool boiling heat transfer coefficient for the copper tube. Furthermore, based on the experimental results, it is not recommended to use nanofluids for enhancing the heat transfer coefficient around the copper surfaces. In conclusion, in terms of quantity, for Al_2O_3 nanoparticles, heat transfer coefficient enhancement of about 47 % is reported for stainless steel tube, and 33 % is reported for brass tube. However, for TiO_2 nanoparticles, heat transfer coefficient enhancement of about 45 % is reported for stainless steel tube, and 29 % for brass tube. In contrast, for copper tube, Al_2O_3, reduction of about 35 %, and TiO_2, reduction of about 48 % is reported.

Nomenclature

A – area, m^2
I – current, A
K – thermal conductivity, W m^{-1} K^{-1}
q – heat, W
r_o – outer radius of cylinder, m
r_i – inner radius of cylinder, m
T – temperature, K
W – power, J s^{-1}
x – liquid mass or mole fraction
y – vapor mass or mole fraction

Subscripts

b – bulk
i – component
id – ideal
l – liquid
s – saturated or surface
th – thermocouples
v – vapor

Greek symbols

α – heat transfer coefficient, W m^{-2} K^{-1}

References

1. *Choi, S.,* Enhancing thermal conductivity of fluids with nanoparticles. Developments and Applications of Non-Newtonian Flows, ASME, FED-Vol. 231/ MD-Vol. 66 1995, pp. 99–105.
2. *Alavi Fazel, A. S., Jamialahmadi, M., Safekordi, A. A.,* Chinese Journal of Chemical Engineering **17** (4) (2009).
3. *Choi, S. U. S,* ASME, FED, 231/MD, **66** (1995) 99.
4. *Das, S. K., Putra, N., Roetzel, W.,* Int. J. Multiph. Flow **29** (2003) 1237.
5. *Das, S. K., Putra, N., Roetzel, W.,* Int. J. Heat Mass Trans. **46** (2003) 851.
6. *You, S. M., Kim, J. H., Kim, K. H.,* Appl. Phys. Lett. **83** (2003) 3374.
7. *Witharana, S.,* Boiling of Refrigerants on Enhanced Surfaces and Boiling of Nanofluids, Ph.D. thesis, Royal Institute of Technology, Stockholm, Sweden, 2003.
8. *Vassllo, P., Kumar, R., Amico, S. D.,* Int. J. Heat Mass Trans. **47** (2004) 407.
9. *Tu, J. P., Dinh, N., Theofanous, T.,* An Experimental Study of Nanofluid Boiling Heat Transfer, in: Proceedings of 6th International Symposium on Heat Transfer, Beijing, China, 2004.
10. *Soltani, S., Etemad, S. G. H., Thibault, J.,* International Communications in Heat and Mass Transfer, Elsevier, (2009).
11. *Ahmed, O., Hamed, M. S.*, The effect of experimental techniques on the pool boiling of nanofluids. 7th International Conference on Multiphase Flow, ICMF 2010, Tampa, Fl, USA 2010.
12. *Alavi Fazel, A. S., Jamialahmadi, M., Safekordi, A. A.,* Chinese Journal of Chemical Engineering **17** (4) (2009).
13. *Alavi Fazel, S. A., Jamialahmadi, M., Safekordi, A. A.,* Iranian J. Chemistry and Chem. Eng. **27** (3) (2008) 135.
14. *Coursey, J. S., Kim, J.,* Int. J. Heat Fluid Flow **29** (2008) 1577.
15. *Kathiravan, R., Kumar, R., Gupta, A., Chandra, R.,* Int. J. Heat and Mass Transfer **53** (2010) 1673.
16. *Suriyawong, A., Wongwises, S.,* ETFS **34** (2010) 992.
17. *Godson L., Raja B., Lal D. M.*, Wongwises S. **14** (2010) 629–641.
18. *Taylor, R. A., Phelan, P. E.,* Int. J Heat and Mass Transfer **52** (2009) 5339.
19. *Cieslinski, J., Kaczmarczyk, T. Z.*, J. of Nano Express, **6** (2011) 220.
20. *Jones, B., Mc Hale, J. P., Garimella, S.,* The Influence of Surface Roughness on Nucleate Pool Boiling Heat Transfer, Birck Nanotechnology Center, Birck and NCN Publications, 2009.